phys. stat. sol. (a) **163**, 475 (1997)

Subject classification: 72.20.Dp; 72.20.Fr; S5.11

Efficient Evaluation of Ionized-Impurity Scattering in Monte Carlo Transport Calculations

H. KOSINA

Institute for Microelectronics, TU Vienna, Gusshausstrasse 27–29, A-1040 Vienna, Austria (phone: ++43/1/58801-3719, fax: ++43/1/5059224, e-mail: kosina@iue.tuwien.ac.at)

(Received June 3, 1997; in revised form July 9, 1997)

Carrier scattering by ionized impurities is strongly anisotropic, and events with small scattering angles are highly preferred. On the Monte Carlo technique applied to semiconductor device modeling this behavior imposes several problems which are discussed. We present a method which reduces the amount of low-angle scattering very effectively. Instead of the anisotropic scattering mechanism an equivalent isotropic mechanism is defined which gives the same momentum relaxation time. Depending on doping concentration and carrier energy the equivalent scattering rate is up to four orders of magnitude lower. By analyzing the Boltzmann transport equation a condition is derived on which the use of the equivalent scattering model is justified. The equivalence of the anisotropic and the isotropic scattering models is also demonstrated empirically by means of Monte Carlo calculations. The plain Brooks-Herring model is employed as well as an improved model including momentum-dependent screening and coherent multi-potential scattering. An empirical correction to attenuate the peak of the scattering rate at low energies is presented, and the statistical screening model of Ridley is critically discussed.

1. Introduction

To simulate carrier transport in submicrometer-scale semiconductor devices the Monte Carlo technique has found widespread application [1 to 4]. Because of high doping concentrations in such devices carrier mobilities are considerably reduced by scattering off ionized impurities.

The large range of Coulomb forces makes the scattering cross section of a single ion very large, or even infinite if no screening is assumed. Therefore, Coulomb scattering is a strongly anisotropic process with a high probability for small-angle scattering events. While scattering events changing the momentum very little are predicted to occur frequently their effect on momentum relaxation is small. This property of Coulomb scattering, though being physically sound, poses some problems on the Monte Carlo technique. A great many of low-angle scattering events have to be processed thus consuming computation time. Very short free-flight times are obtained which further degrade the efficiency of the Monte Carlo procedure.

Fig. 1 illustrates this problem. As an example, the low-field mobility as a function of the ionized-impurity concentration, N_I, has been calculated by the Monte Carlo method. The standard Brooks-Herring model was employed (see, e.g. [5][6]). One can observe that at low impurity concentrations about 93% of all scattering events are of Coulomb type. Phonon scattering constitutes the rest. The curve in Fig. 1 then decreases slightly with increasing N_I and at about 10^{20} cm^{-3} starts to increase. The latter effect is due to degeneracy when the power law of the screening parameter β_s changes from $N_\mathrm{I}^{1/2}$ to

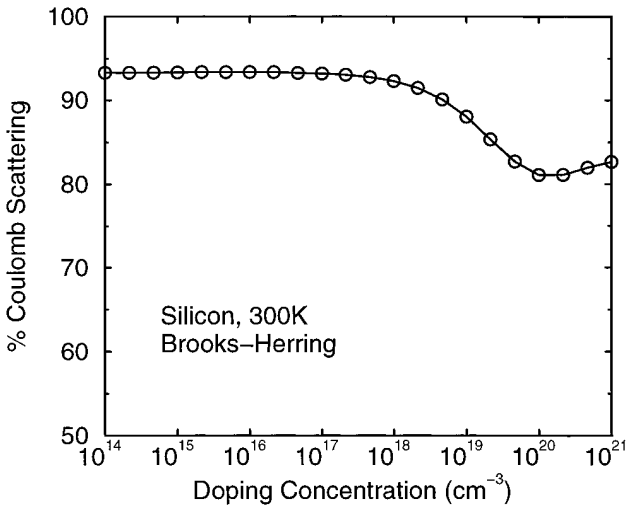

Fig. 1. Relative frequency of Coulomb scattering as a function of doping concentration. Because of the large range of Coulomb forces the frequency is very high even at low concentrations

$N_{\mathrm{I}}^{1/6}$. At low impurity concentrations we observe the paradoxical situation that on the one hand ionized-impurity scattering is the most frequent process, and that on the other hand it has nearly no effect on the mobility. This discrepancy occurs because the collisional and the momentum cross sections for the considered process can differ by several orders of magnitude.

We present a method which allows to reduce the amount of low-angle scattering very efficiently without altering the underlying transport problem. Instead of using the highly anisotropic scattering cross section of screened Coulomb interaction we use an equivalent cross section, which is isotropic, and which yields the same the momentum relaxation rate as the anisotropic cross section. A condition is derived on which the use of the equivalent cross section is justified.

Another advantage of the new scattering model is that it is well suited for full-band Monte Carlo calculations. In these calculations it is problematic to randomly select a momentum transfer q according to a non-constant probability density function. This specific problem does not arise if an equivalent isotropic model is used instead of the original anisotropic one.

2. Mobility Definition

The transport properties of carriers in semiconductors can be well described by the Boltzmann transport equation [7]. In the following we consider the scattering integral at the right-hand side of the Boltzmann equation which takes for the non-degenerate case the form

$$\left(\frac{\partial f}{\partial t}\right)_c = \frac{V_0}{(2\pi)^3}\int_{\mathbf{k}} \{P(\mathbf{k}',\mathbf{k})f(\mathbf{k}') - P(\mathbf{k},\mathbf{k}')f(\mathbf{k})\}\,\mathrm{d}\mathbf{k}'\,. \tag{1}$$

Here, V_0 denotes the volume of the crystal, f is the electron distribution function and $\mathbf{k}$ the electron wave vector. Scattering of charge carriers is a quantum mechanical process

which is frequently treated by quantum mechanical perturbation theory. $P(\mathbf{k},\mathbf{k}')$ in (1) represents the transition probability from an initial state $\mathbf{k}$ to a final state $\mathbf{k}'$.

A macroscopic momentum balance equation is obtained by multiplying both sides of the Boltzmann equation by the electron momentum, $\mathbf{p} = \hbar\mathbf{k}$, and integrating over $\mathbf{k}$. By applying this procedure to (1) one obtains the average rate of loss of electron momentum due to scattering

$$\left(\frac{\partial \mathbf{p}}{\partial t}\right)_c = \int_{\mathbf{k}} \hbar\mathbf{k}\left(\frac{\partial f}{\partial t}\right)_c \mathrm{d}\mathbf{k} \tag{2}$$

$$= -\hbar \int_{\mathbf{k}} f(\mathbf{k}) \left(\frac{V_0}{(2\pi)^3} \int_{\mathbf{k}'} (\mathbf{k}-\mathbf{k}')\, P(\mathbf{k}',\mathbf{k})\, \mathrm{d}\mathbf{k}' \right) \mathrm{d}\mathbf{k} \tag{3}$$

$$= -\hbar \int_{\mathbf{k}} f(\mathbf{k})\, \mathbf{k}\, \tau_{\mathrm{m}}^{-1}(\mathbf{k})\, \mathrm{d}\mathbf{k}\,. \tag{4}$$

In order to proceed from (3) to (4) one has to assume that P depends only on θ, the angle between $\mathbf{k}$ and $\mathbf{k}'$, and not on the azimuthal angle φ,

$$P(\mathbf{k},\mathbf{k}') \equiv P(k,k',\cos\theta)\,. \tag{5}$$

This assumption is fulfilled for any isotropic scattering potential. The condition (5) ensures that the vector-valued integral over $\mathbf{k}'$ in (3) is parallel to $\mathbf{k}$, and the proportionality factor between these two vectors is given by the microscopic momentum relaxation time, τ_{m}.

Now we introduce as defining relation for the mobility (see, e.g. [8][9])

$$\mathbf{J} = -\mu\left(\frac{\partial \mathbf{p}}{\partial t}\right)_c\,. \tag{6}$$

In this general form, μ is a tensor quantity. Due to an anisotropic band structure and an arbitrarily distorted off-equilibrium distribution function the current density and the momentum loss rate are not necessarily parallel vectors. The electron current density is defined as

$$\mathbf{J} = -e \int_{\mathbf{k}} \mathbf{v}_{\mathrm{g}}(\mathbf{k})\, f(\mathbf{k})\, \mathrm{d}\mathbf{k}\,. \tag{7}$$

A scalar mobility can finally be extracted from (6) by using the magnitudes of the involved vectors,

$$\mu = \frac{\left|\int e\, \mathbf{v}_{\mathrm{g}}(\mathbf{k})\; f(\mathbf{k})\; \mathrm{d}\mathbf{k}\right|}{\left|\int \hbar\, \mathbf{k}\; \tau_{\mathrm{m}}^{-1}(\mathbf{k})\; f(\mathbf{k})\; \mathrm{d}\mathbf{k}\right|}\,. \tag{8}$$

In the following we adopt this mobility definition because its derivation involves only very few approximations. Other mobility definitions found in the literature rely on much more stringent assumptions, such as the relaxation time approximation, constant effective mass, and/or a perturbative solution of the Boltzmann equation at very low electric fields.

3. The Equivalent Scattering Cross Section

Anisotropic and elastic scattering can be discussed in terms of the differential scattering cross section, $\sigma(k, \cos\theta)$. For a given wave number k, the differential scattering cross section can be interpreted as a probability density function of the scattering angle θ. In the following the notation notation $z = \cos\theta$ will be adopted. For ionized-impurity scattering the differential scattering cross section σ and the quantum mechanical transition probability P are related by (see, e.g. [5])

$$\sigma(k,z) = \frac{1}{N_\mathrm{I}\, v_\mathrm{g}(k)} \frac{V_0}{(2\pi)^3} \int_0^\infty P(k,k',z) k'^2 \,\mathrm{d}k' \,. \tag{9}$$

N_I denotes the concentration of the impurity centers, and v_g is assumed to be derived from an isotropic band structure, $v_\mathrm{g} = \partial E/\partial\hbar k$. The total scattering rate λ and the momentum relaxation time, which was introduced in (4), can be expressed in terms of the differential scattering as follows:

$$\lambda(k) = 2\pi\, N_\mathrm{I}\, v_\mathrm{g}(k) \int_{-1}^{1} \sigma(k,z)\,\mathrm{d}z\,, \tag{10}$$

$$\frac{1}{\tau_\mathrm{m}(k)} = 2\pi\, N_\mathrm{I}\, v_\mathrm{g}(k) \int_{-1}^{1} (1-z)\,\sigma(k,z)\,\mathrm{d}z\,. \tag{11}$$

To tackle the problem of small-angle scattering we construct an equivalent scattering cross section $\tilde{\sigma}$ that fulfills two requirements:

1. The equivalent cross section is isotropic:

$$\frac{\partial\tilde{\sigma}(k,z)}{\partial z} \equiv 0\,; \tag{12}$$

2. The equivalent and the original cross section yield identical momentum relaxation times:

$$\tilde{\tau}_\mathrm{m}(k) \equiv \tau_\mathrm{m}(k)\,. \tag{13}$$

With (13) it is ensured that the main transport parameter, namely the non-equilibrium mobility (6), is not altered as long as the distribution function remains unchanged.

The scattering cross section $\tilde{\sigma}$ and the total scattering rate $\tilde{\lambda}$ of the equivalent model can readily be obtained by combining (10), (11) and (12), (13)

$$\tilde{\sigma}(k,z) \equiv \tilde{\sigma}(k) = \frac{1}{2} \int_{-1}^{1} (1-z')\,\sigma(k,z')\,\mathrm{d}z'\,, \tag{14}$$

$$\tilde{\lambda}(k) = \frac{1}{\tau_\mathrm{m}(k)} \tag{15}$$

In a Monte Carlo procedure ionized-impurity scattering can now be treated as an elastic and isotropic process. The scattering rate for this process is given by (15). The computation of after-scattering state, **k'**, is considerably simplified due to the isotropicity of the

process

$$k' = k\,, \qquad \varphi' = 2\pi r_1\,, \qquad \cos\theta' = 2r_2 - 1\,,$$

where r_1 and r_2 are two random numbers evenly distributed between 0 and 1, and spherical polar coordinates are assumed.

For an anisotropic scattering process with a high preference for forward scattering the momentum relaxation rate τ_{m}^{-1} is always smaller than the total scattering rate λ. Therefore, using the equivalent scattering rate (15) in a Monte Carlo procedure has the advantage that ionized-impurity scattering becomes a less frequent scattering process. The effect, that the equivalent scattering model requires a considerably lower number of Coulomb scattering events to be processed, can be interpreted as a gathering of many scattering events each with small momentum transfer to one scattering event with large momentum transfer.

Now the question arises to what extent the transport problem is altered when the equivalent scattering model is used. We assume that the transport problem is described by a Boltzmann equation. Because any change of the scattering cross section will not change the left-hand side of this equation, we only have to investigate how the right-hand side is affected. In the Appendix we show that the scattering integrals are identical,

$$\left(\widetilde{\frac{\partial f}{\partial t}}\right)_c \equiv \left(\frac{\partial f}{\partial t}\right)_c \tag{16}$$

if two prerequisites are fulfilled. First, the transition probability P has to account for exact energy conservation as it is stated by the δ–function in the golden rule of Fermi. Second, the distribution function has to be of the following form which is usually referred to as diffusion approximation

$$f(k, \cos\theta) = f_{\mathrm{S}}(k) + f_1(k)\cos\theta\,. \tag{17}$$

The impact of this restriction is supposed to be practically negligible for the here considered problems. One should be aware of the fact that λ and P in the scattering integral (1) comprise contributions of many scattering processes, and that only the contribution of Coulomb scattering is eventually modified but not those of the dominant phonon processes. Furthermore, Coulomb scattering plays an important role especially at low electric fields, where the approximation (17) is certainly very accurate. At high fields, however, where it might become necessary to include higher powers of $\cos\theta$ in (17) the influence of Coulomb scattering diminishes rapidly. For instance, the saturation velocity does not depend on the doping concentration and hence not on impurity scattering.

For the reasons discussed so far it can be expected that replacing a particular anisotropic Coulomb scattering model by the corresponding isotropic one will introduce an error which is virtually negligible in most practical cases.

4. Ridley's Statistical Screening Model

One subject to be discussed in the context of the problems related to small-angle scattering is the statistical screening model introduced by Ridley [10]. In a form suited for Monte Carlo calculations [11] this model has become very popular, and many authors have employed it in their Monte Carlo codes.

Formally, the statistical screening model is obtained by modifying the scattering cross section of the Brooks-Herring model as follows:

$$\sigma_{mod}(k,z) = \sigma_{\mathrm{BH}}(k,z)\exp(-RN_{\mathrm{I}}\pi b^2(z))\,, \tag{18}$$

R denotes the average distance between the ions, and b is the impact parameter as function of the scattering angle, $z = \cos\theta$. This model can be interpreted to cut off the long-range part of the screened Coulomb interaction. As a consequence the amount of low-angle scattering is effectively reduced, which is probably the main reason for the popularity of this model. However, it is to note that according to (11) and (6) such modification of the cross section inevitably results in a modified mobility.

The original intention was to get an impurity scattering model that is applicable over a wide range of conditions. However, in a semiconductor at finite temperature we have a more specific condition in that free carriers responsible for screening are always available. Therefore, in the case of semiconductors it is not necessary to bridge the gap between the Conwell-Weisskopf (see, e.g. [5][6]) and the Brooks-Herring models, and the latter model can always be used without facing any divergence problems.

We now shall briefly discuss the basic assumptions of the Brooks-Herring model and the additional assumption introduced by the concept of statistical screening. For the Brooks-Herring model the transition probability is derived for one screened impurity center in the Born approximation. Then the situation in a doped semiconductor is described by simply multiplying the single-center transition probability by the total number of impurities, $N_{\mathrm{I}}V_0$.

Especially this procedure of weighting all centers equally is not adopted in Ridley's model. Ridley argues that the random location of the impurities leads to some extent to statistical cancellation of the many impurity potentials. With the scattering cross section a weight has to be assigned which decreases exponentially with the distance of the electron from the impurity center ((18)). A measure for this distance is the impact parameter.

However, the introduction of such an exponential weight function appears somewhat artificial, and we think of two indications that suggest that all the impurity centers should be weighted equally. First, it seems that, instead of leading to weaker scattering due to statistical screening, the random location of the centers is a prerequisite to have effective Coulomb interaction. In [12] experimental evidence is reported that scattering becomes weaker if part of the ionized centers are correlated. If all impurities formed some regular pattern there would be no impurity scattering at all. Therefore, assuming that non-correlated impurities lead to weaker scattering seems not logical.

Second, one can consider the potential caused by all impurities. Within the linear screening theory the screened Coulomb potentials V_{s} of the single centers can be superimposed in a straightforward manner,

$$V(\mathbf{r}) = V_{\mathrm{s}}(\mathbf{r}-\mathbf{r_1}) + V_{\mathrm{s}}(\mathbf{r}-\mathbf{r_2}) + \dots \tag{19}$$

Using the Born approximation the Fourier transform of the potential has to be calculated and the absolute value of the squared potential. The linear translations of the potentials only change the phase.

$$V(\mathbf{q}) = V_{\mathrm{s}}(q)\exp(-i\mathbf{q}\cdot\mathbf{r_1}) + V_{\mathrm{s}}(q)\exp(-i\mathbf{q}\cdot\mathbf{r_2}) + \dots\,, \tag{20}$$

$$|V(\mathbf{q})|^2 = |V_{\mathrm{s}}^2(q)| + |V_{\mathrm{s}}^2(q)| \dots + 2|V_{\mathrm{s}}^2(q)|\cos(\mathbf{q}\cdot(\mathbf{r_2}-\mathbf{r_1})) + \dots\,. \tag{21}$$

Obviously, the single-ion contributions in (21) do not depend on any spatial coordinate. Only the interference terms containing the cosine function depend on the spatial locations of the ions. These terms describe coherent two-ion scattering. Both the Brooks-Herring model and Ridley's model explicitly treat scattering as two-body interactions. Therefore, when discussing these models we have to consider only the single-ion terms in (21) and can exclude the two-ion terms from the discussion. We conclude from (21) that for any single-ion scattering model the single-ion potentials have to be superimposed with unity weight.

5. Ionized Impurity Scattering

We start with the Brooks-Herring model and then discuss some physical refinements of this model. For the Brooks-Herring model the Fourier transform of the scattering potential is of the form

$$|V_{\mathrm{BH}}(q)|^2 = \left(\frac{Ze}{\varepsilon_0 \varepsilon_\mathrm{r}}\right)^2 \frac{1}{(q^2+\beta_\mathrm{s}^2)^2} \,, \tag{22}$$

where ε_r denotes the relative permittivity of the semiconductor, and β_s is the inverse Fermi-Thomas screening length,

$$\beta_\mathrm{s}^2 = \frac{e^2 n}{\varepsilon_0 \varepsilon_\mathrm{r} k_\mathrm{B} T_n} \frac{\mathcal{F}_{-1/2}(\eta)}{\mathcal{F}_{1/2}(\eta)} \,. \tag{23}$$

Here, n represents the electron concentration, T_n the electron temperature, $\mathcal{F}_j$ the Fermi integral of order j, and η is the reduced Fermi energy. Employing the potential (22) in Fermi's golden rule and performing the integration over the final states one ends up with a scattering rate λ_{BH} and a momentum relaxation rate, which defines the equivalent scattering rate $\tilde{\lambda}_{\mathrm{BH}}$,

$$\lambda_{\mathrm{BH}}(k) = C(k) \frac{1}{2\beta_\mathrm{s}^2} \frac{b}{1+b} \,, \tag{24}$$

$$\tilde{\lambda}_{\mathrm{BH}}(k) = C(k) \frac{1}{4k^2} \left(\ln(1+b) - \frac{b}{1+b} \right) . \tag{25}$$

In these equations we have set $b = 4k^2/\beta_\mathrm{s}^2$, and the energy-dependent prefactor C is of the form

$$C(k) = \frac{N_\mathrm{I} Z^2 e^4}{2\pi\hbar^2 (\varepsilon_0 \varepsilon_\mathrm{r})^2 v_\mathrm{g}(k)} \,. \tag{26}$$

Fig. 2 shows the ratio $\tilde{\lambda}_{\mathrm{BH}}/\lambda_{\mathrm{BH}}$ as a function of the doping concentration for a low-energetic electron ($E = 0.1 k_\mathrm{B} T$), a thermal electron ($E = k_\mathrm{B} T$) and a hot electron ($E = 10 k_\mathrm{B} T$). Depending on the doping concentration and the electron energy the scattering rate of the isotropic model can be several orders of magnitude lower than that of the anisotropic model. This results in a considerable saving of time expended at the processing of Coulomb scattering events in the course of a Monte Carlo calculation.

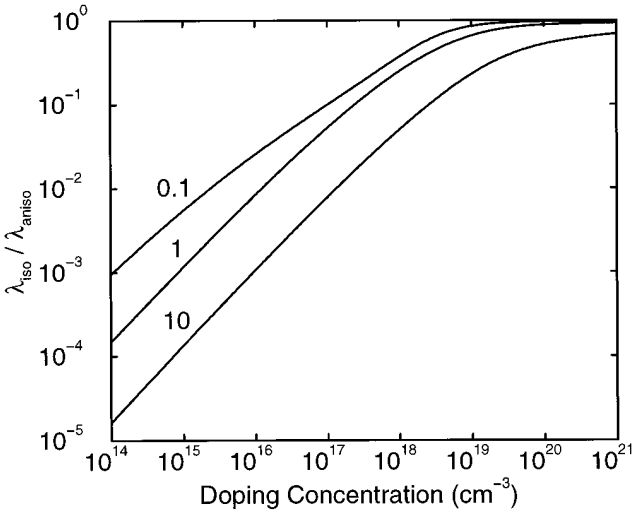

Fig. 2. Ratio of the isotropic scattering rate, which is equal to the momentum relaxation rate, and the anisotropic scattering rate as it results from the Brooks-Herring model (Eqs. (24) and (25)). The parameter denotes the electron energy normalized by $k_{\mathrm{B}}T$, with $T = 300$ K

The Brooks-Herring model is well suited to demonstrate the peculiarities of ionized-impurity scattering. To get quantitative agreement with measured mobility curves, however, the model needs to be extended to include additional physical effects. We found that momentum-dependent screening and a correction term for coherent multi-ion scattering have a strong impact on the mobility. How these effects can be accounted for in an uncomplicated fashion will be published elsewhere. The resulting scattering potential is given by

$$|V(q)|^2 = \left(\frac{Ze}{\varepsilon_0 \varepsilon_{\mathrm{r}}}\right)^2 \frac{1}{\left(q^2 + \beta_{\mathrm{s}}^2 G(q)\right)^2} \left(1 + \frac{\sin qR}{qR}\right) . \tag{27}$$

Here, R denotes the average distance between ions which is defined as $R = (2\pi N_{\mathrm{I}})^{-1/3}$. The screening function G is approximated by a rational function [13].

The model of ionized-impurity scattering defined by (27) can be employed in a Monte Carlo procedure very efficiently by resorting to internal self-scattering. Within this framework scattering is treated as if it were a Brooks-Herring problem. The Brooks-Herring scattering rate is multiplied by some amplification factor B, which is chosen such that the following inequality is fulfilled in the interval $q \in [0, 2k]$:

$$B|V_{\mathrm{BH}}(q)|^2 \geq |V(q)|^2 . \tag{28}$$

In this way we get a Brooks-Herring type scattering rate which is larger than the scattering rate $\tilde{\lambda}$ resulting from the potential (27),

$$B\tilde{\lambda}_{\mathrm{BH}}(k) \geq \tilde{\lambda}(k) . \tag{29}$$

Note that both $\tilde{\lambda}_{\mathrm{BH}}$ and $\tilde{\lambda}$ are rates of isotropic scattering processes. Now there is a well-defined probability P of accepting the selected scattering event: $P = \tilde{\lambda}/B\tilde{\lambda}_{\mathrm{BH}}$. This prob-

ability can also be expressed as

$$P = \frac{\int_0^{2k} |V(q)|^2 q^3 \mathrm{d}q}{B \int_0^{2k} |V_{\mathrm{BH}}(q)|^2 q^3 \mathrm{d}q} \quad . \tag{30}$$

Instead of solving these integrals directly one can think of solving them by means of Monte Carlo integration. Keeping this in mind the internal self-scattering algorithm can be defined as follows. A random number $q_{\mathrm{r}} \in [0, 2k]$ is chosen according to the probabil-

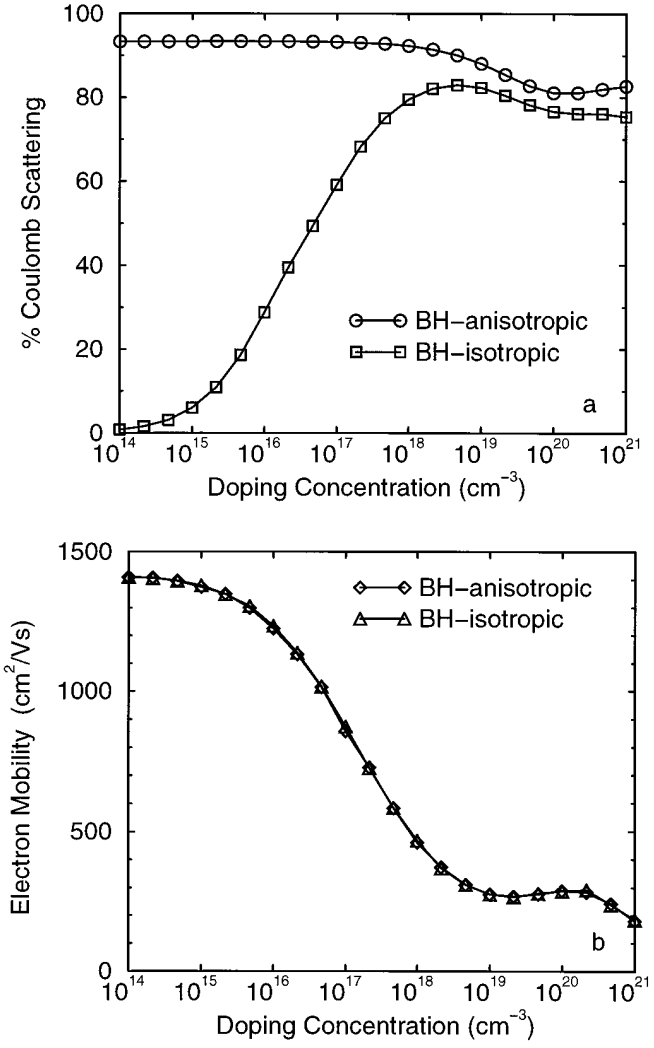

Fig. 3 Comparison of the a) relative frequencies and b) low-field mobilities obtained from the anisotropic Brooks-Herring model and the equivalent isotropic model; $T = 300$ K and $E = 700$ V/cm

ity density function $|V_{\mathrm{BH}}(q)|^2 q^3$. Then a random number p_{r} is chosen evenly distributed between 0 and $B|V_{\mathrm{BH}}(q_{\mathrm{r}})|^2$. If $p_{\mathrm{r}} < |V(q_{\mathrm{r}})|^2$ then the scattering event is accepted, otherwise it is rejected and self-scattering is performed instead.

By means of the described method explicit integration of the potential (27) can be avoided, a task which can be very time-consuming depending on the complexity of the used screening function.

6. Results and Discussion

The low-field mobility in uncompensated silicon will be discussed. In addition to ionized-impurity scattering the transport model comprises acoustic intra-valley scattering, six different types of phonon inter-valley scattering [6] and plasmon scattering. We adopt a non-parabolic and isotropic band structure using an effective mass of $m^* = 0.32$ and a non-parabolicity coefficient of $\alpha = 0.5\ \mathrm{eV}^{-1}$. Room temperature is assumed.

A single-particle Monte Carlo program is employed, and steady-state averages are computed by sampling the quantities of interest at the before-scattering states [6]. Due to the high carrier concentrations considered the Pauli exclusion principle has to be accounted for. A rejection technique [6] is used assuming equilibrium Fermi-Dirac statistics for the occupation probabilities of the final states. The electron mobility presented in the following is given by $\mu = v_{\mathrm{d}}/E$, where the drift velocity, $v_{\mathrm{d}} = \langle v_{\mathrm{g}} \rangle$, is obtained by averaging the electron group velocity, and the assumed magnitude of the electric field was 700 V/cm. It should be noted that (6), which was used to theoretically justify the new approach, will consistently simplify to $\mu = v_{\mathrm{d}}/E$ if a spatially uniform condition is assumed.

In Fig. 3 the anisotropic Brooks-Herring model (24) and the equivalent isotropic model (25) are compared. Fig. 3a shows that the isotropic scattering model considerably

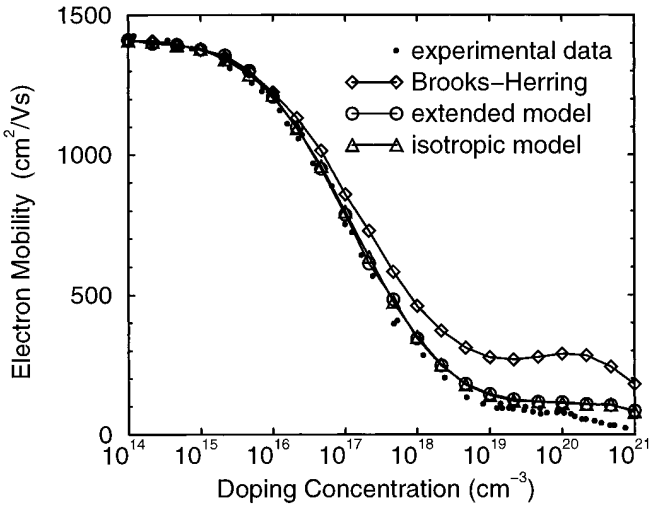

Fig. 4. Results of the Brooks-Herring model and the extended Coulomb scattering model compared with experimental data [14]. The extended model agrees better with the experimental data than the plain Brooks-Herring model. Both, the anisotropic version and the isotropic version of the extended model yield the same results

reduces the amount of Coulomb scattering events, especially at low doping concentrations. Despite the large difference in the frequency of Coulomb scattering Fig. 3b demonstrates that the resulting concentration-dependent mobilities are virtually identical. This result confirms the theoretical investigations in Section 3.

The mobilities resulting from the scattering potential (27) are plotted in Fig. 4. This potential gives significantly better agreement with experimental data [14] than the plain Brooks-Herring model, which considerably overestimates the mobility at intermediate and high doping concentrations. Scattering caused by the potential (27) has been implemented both as an anisotropic model and as an equivalent isotropic model. The algorithm for the isotropic model was further simplified by using internal self-scattering as reported in the previous section. Fig. 4 shows that both ways of implementing the scattering model yields identical results.

Finally, we shall discuss the peculiar energy dependence of Coulomb scattering and how to overcome the related problems. In Fig. 5 the Brooks-Herring scattering rate is plotted as a function of the energy. Characteristic of Coulomb scattering is the peak at low energies which is located around $E_\beta/4$ and increases with decreasing doping concentration. E_β defined as $E_\beta = \hbar^2\beta_s^2/2m^*$ is on the order of 0.02 meV at $N_I = 10^{16}$ cm^{-3}. This energy is by more than four orders of magnitude smaller than the thermal energy ($k_BT = 25.8$ meV at room temperature). According to the thermal distribution there will be only few electrons that are affected by this peak of the scattering rate. Unfortunately, not only the scattering rate but also the momentum relaxation rate shows such a peak at low energies (Fig. 5).

We introduce an empirical correction to attenuate this peak and hence to remove the necessity of dealing with extraordinarily high scattering frequencies in Monte Carlo simulations. We start with the statistical screening model of Ridley. The modified cross

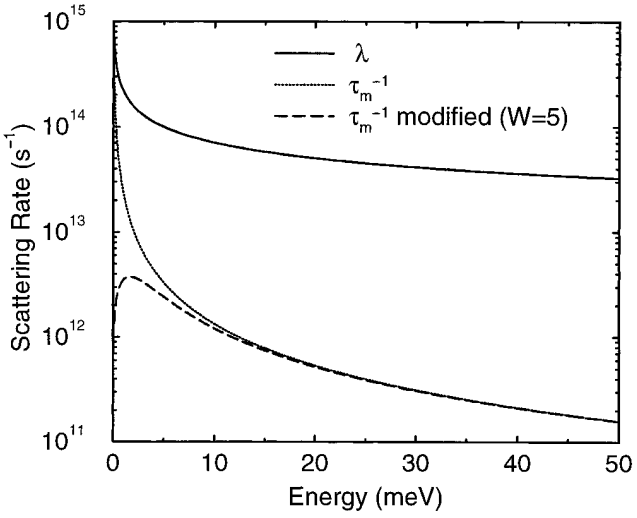

Fig. 5 Scattering rate according to the Brooks-Herring model and the corresponding momentum relaxation rate at $N_I = 10^{15}$ cm^{-3} and $T = 300$ K. An empirical correction is used to attenuate the peak at low energies

section (18) results in the following modified scattering rate [11]:

$$\lambda_{\mathrm{mod}}(k) = \frac{v_{\mathrm{g}}(k)}{R}\left(1 - \exp\left(-\lambda_{\mathrm{BH}}(k)\frac{R}{v_{\mathrm{g}}(k)}\right)\right). \tag{31}$$

This rate does not show the problematic behavior at low energies. One can think that the expression $v_{\mathrm{g}}(k)/R$ defines some maximum rate λ_{max} and that (31) is a rule that ensures that λ_{mod} is always smaller than λ_{max}. Eq. (31) satisfies the following inequality:

$$\lambda_{\mathrm{mod}}(k) \leq \mathrm{Min}\{\lambda_{\mathrm{max}}(k), \lambda_{\mathrm{BH}}(k)\}. \tag{32}$$

We now chose some maximum rate λ_{max} to artificially limit the physically correct scattering rate λ. A simple rule which fulfills condition (32), and which is symmetric with respect λ and λ_{max}, is the harmonic mean

$$\frac{1}{\lambda_{\mathrm{mod}}} = \frac{1}{\lambda_{\mathrm{max}}} + \frac{1}{\lambda}. \tag{33}$$

Obviously, the larger λ_{max} is taken the more λ_{mod} resembles the physically correct rate λ. λ_{max} is an artificial quantity which has to be chosen such that the effect on measured quantities such as the mobility is negligible. Purely empirically we assume

$$\lambda_{\mathrm{max}}(k) = W v_{\mathrm{g}}(k)\beta_{\mathrm{s}}. \tag{34}$$

Monte Carlo simulations revealed that relative to the plain Brooks-Herring model the increase in low-field mobility due to the modification (33) is less than 1.5% for $W = 10$ and less than 2.3% for $W = 5$. For comparison, Ridley's statistical screening model yields low-field mobility enhancements up to 9%, depending on the doping concentration. Therefore, to keep any empirical modification of the mobility as low as possible one should use the modified rate (33) with an appropriate choice for W instead of the rate (31).

7. Conclusion

A method has been presented which effectively reduces the amount of low-angle scattering events that have to be processed during a Monte Carlo transport calculation. The inverse momentum relaxation time serves as scattering rate for an equivalent scattering model. The equivalent model, which is isotropic, exhibits an up to four orders of magnitude lower scattering rate, depending on doping concentration and carrier energy. An analysis of the scattering integral of the Boltzmann transport equation indicates that using the equivalent isotropic model instead of the anisotropic one has negligible influence on the transport problem of charge carriers in semiconductors. Monte Carlo calculations demonstrated the equivalence of both types of scattering models empirically. The assumptions of the statistical screening model of Ridley are critically examined, and we found that the predictions regarding mobility made by this model go into the wrong direction. To deal with the peak of the scattering rate at low energies we presented an empirical correction whose effect on the mobility can be controlled by a free parameter.

Acknowledgements The author would like to thank G. Kaiblinger-Grujin for many fruitful discussions, and S. Selberherr for continued encouragement.

Appendix

The scattering integral (1) can be rewritten for a φ-independent transition probability.

$$\left(\frac{\partial f}{\partial t}\right)_c = -\lambda(k) f(\mathbf{k}) + \frac{V_0}{(2\pi)^3} \int_0^\infty k'^2 \mathrm{d}k' \int_{-1}^{1} \mathrm{d}z' \; P(k,k',z') \int_0^{2\pi} \mathrm{d}\varphi' f(k',z',\varphi') \,. \tag{35}$$

Furthermore, for the transition probability P Fermi's golden rule shall hold

$$P(\mathbf{k}',\mathbf{k}) = \frac{2\pi}{\hbar} |M(\mathbf{q})|^2 \; \delta(E - E') \,. \tag{36}$$

The isotropic cross section: As a first step we evaluate (35) for the equivalent scattering model which is isotropic. From (9), (14) and the golden rule (36) one can derive some artificial matrix element $\tilde{M}$ which can be assigned to the equivalent scattering model.

$$\tilde{M}^2(k) = \frac{1}{2} \int_{-1}^{1} (1-z) \; M^2(q(k,z)) \; \mathrm{d}z \,. \tag{37}$$

For an elastic scattering mechanism as considered here the momentum transfer is given by $q^2(k,z) = 2k^2(1-z)$. Keeping in mind that the transition probability $\tilde{P}$ is independent of z the scattering integral (35) can be written as

$$\widetilde{\left(\frac{\partial f}{\partial t}\right)}_c = -\tilde{\lambda}(k) f(\mathbf{k}) + \frac{V_0}{(2\pi)^3} \int_0^\infty \tilde{P}(k',k) \; k'^2 \mathrm{d}k' \int_{-1}^{1} \mathrm{d}z' \int_0^{2\pi} \mathrm{d}\varphi' \; f(k',z',\varphi') \;\; . \tag{38}$$

The integral of f over the unit sphere yields the spherically symmetric part of f,

$$f_\mathrm{S}(k) = \frac{1}{4\pi} \int_{-1}^{1} \mathrm{d}z \int_0^{2\pi} \mathrm{d}\varphi \; f(k,z,\varphi) \,. \tag{39}$$

The δ-function within $\tilde{P}$ allows one to put $f_\mathrm{S}(k')$ in front of the integral,

$$\widetilde{\left(\frac{\partial f}{\partial t}\right)}_c = -\tilde{\lambda}(k) \cdot f(\mathbf{k}) + 4\pi \; f_\mathrm{S}(k) \; \frac{V_0}{(2\pi)^3} \int_0^\infty \tilde{P}(k',k) \; k'^2 \mathrm{d}k' \,. \tag{40}$$

The remaining integral evaluates to $\tilde{\lambda}$ so that we end up with

$$\widetilde{\left(\frac{\partial f}{\partial t}\right)}_c = -\tilde{\lambda}(k)(f(\mathbf{k}) - f_\mathrm{S}(k)) \;\; . \tag{41}$$

Without loss of generality the distribution function can be decomposed into a spherically symmetrical and an anisotropic part,

$$f(\mathbf{k}) = f_\mathrm{S}(k) + f_\mathrm{A}(\mathbf{k}) \tag{42}$$

With (15) and (42) we get the following scattering integral for the equivalent model:

$$\left(\widetilde{\frac{\partial f}{\partial t}}\right)_c = -\frac{f_{\mathrm{A}}(\mathbf{k})}{\tau_{\mathrm{m}}(k)} \,. \tag{43}$$

The anisotropic cross section: To be able to evaluate the scattering integral (35) for the anisotropic cross section we have to make the assumption (17) on the shape of the distribution function.

We shall now introduce a spherical polar coordinate system with the polar axis parallel to $\mathbf{k}$. The solid angle of the electric field is denoted by $\mathbf{\Omega} = (\theta, \varphi)$, and that of $\mathbf{k}'$ by $\mathbf{\Omega}' = (\theta', \varphi')$. The angle between the electric field and $\mathbf{k}'$ can then be expressed as

$$\cos\gamma = \cos\theta\cos\theta' - \cos(\varphi - \varphi')\sin\theta\sin\theta' \;. \tag{44}$$

Setting $z = \cos\theta$ and $z' = \cos\theta'$ we obtain

$$\begin{aligned}\left(\frac{\partial f}{\partial t}\right)_c &= -\lambda(k)\; f(k,z) \\ &\quad + \frac{V_0}{(2\pi)^3}\int_0^\infty k'^2\,\mathrm{d}k' \int_0^{2\pi}\mathrm{d}\varphi' \int_{-1}^{1}\mathrm{d}z'\;(f_{\mathrm{S}}(k') + f_1(k')\cos\gamma)\; P(k,k',z')\end{aligned} \tag{45}$$

After integration over φ' and after putting f_{S} and f_1 in front of the integral by employing the δ-function in P one arrives at

$$\begin{aligned}\left(\frac{\partial f}{\partial t}\right)_c &= -\lambda(k)\; f(k,z) \\ &\quad + f_{\mathrm{S}}(k)\;\frac{V_0}{(2\pi)^2}\int_0^\infty k'^2\,\mathrm{d}k' \int_{-1}^{1}\mathrm{d}z'\; P(k,k',z') \\ &\quad + f_1(k)\;\cos\theta\frac{V_0}{(2\pi)^2}\int_0^\infty k'^2\,\mathrm{d}k' \int_{-1}^{1} dz'\; z'\; P(k,k',z') \;.\end{aligned} \tag{46}$$

The first integral on the right-hand side evaluates to $\lambda(k)$, and the second one to $\lambda(k) - \tau_{\mathrm{m}}^{-1}(k)$. In the final result only the anisotropic part of f appears,

$$\left(\frac{\partial f}{\partial t}\right)_c = -\frac{f_1(k)\;\cos\theta}{\tau_{\mathrm{m}}(k)} \,. \tag{47}$$

This results coincides with (43) if the anisotropic part of the distribution function is of the form $f_{\mathrm{A}}(\mathbf{k}) = f_1(k)\cos\theta$.

References

[1] M. FISCHETTI and S. LAUX, Phys. Rev. B **38**, 9721 (1988).
[2] J. HIGMAN, K. HESS, C. HWANG, and R. DUTTON, IEEE Trans. Electron Devices **36**, 930 (1989).
[3] F. VENTURI, R. K. SMITH, E. C. SANGIORGI, M. R. PINTO, and B. RICCO, IEEE Trans. Computer-Aided Design **8**, 360 (1989).

[4] H. Kosina and S. Selberherr, IEEE Trans. Computer-Aided Design **12**, 201 (1994).
[5] D. Chattopadhyay and H. Queisser, Rev. Mod. Phys. **53**, 745 (1981).
[6] C. Jacoboni and P. Lugli, The Monte Carlo Method for Semiconductor Device Simulation, Springer-Verlag, Wien/New York 1989.
[7] S. Selberherr, Analysis and Simulation of Semiconductor Devices, Springer-Verlag, Wien 1984.
[8] S. Bandyopadhyay, M. E. Klausmeier-Brown, C. M. Maziar, S. Datta, and M. Lundstrom, IEEE Trans. Electron Devices **34**, 392 (1987).
[9] S. Lee and T. Tang, Solid State Electronics **35**, 561 (1992).
[10] B. Ridley, J. Phys. C **10**, 1589 (1977).
[11] T. Van de Roer and F. Widdershoven, J. Appl. Phys. **59**, 813 (1986).
[12] E. Buks, M. Heiblum, and H. Shtrikman, Phys. Rev. B **49**, 14790 (1994).
[13] H. Kosina and G. Kaiblinger-Grujin, Solid State Electronics (1997), in print.
[14] G. Masetti, M. Severi, and S. Solmi, IEEE Trans. Electron Devices **30**, 764 (1983).